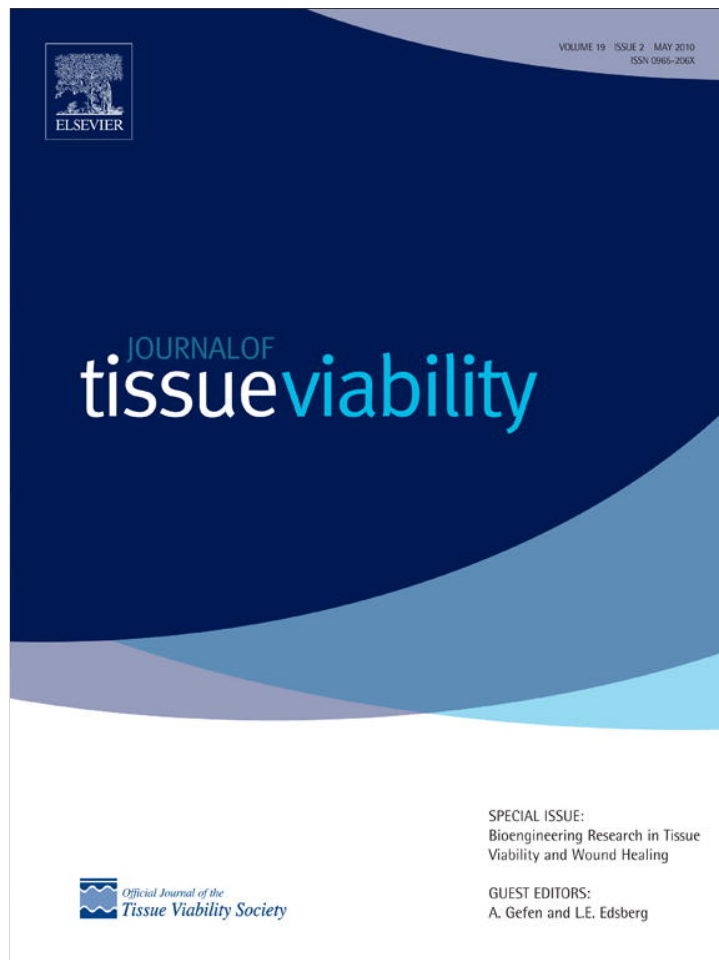


Provided for non-commercial research and education use.  
Not for reproduction, distribution or commercial use.



This article appeared in a journal published by Elsevier. The attached copy is furnished to the author for internal non-commercial research and education use, including for instruction at the authors institution and sharing with colleagues.

Other uses, including reproduction and distribution, or selling or licensing copies, or posting to personal, institutional or third party websites are prohibited.

In most cases authors are permitted to post their version of the article (e.g. in Word or Tex form) to their personal website or institutional repository. Authors requiring further information regarding Elsevier's archiving and manuscript policies are encouraged to visit:

<http://www.elsevier.com/copyright>



ELSEVIER

---



---

 JOURNAL OF  
**tissueviability**


---



---

[www.elsevier.com/locate/jtv](http://www.elsevier.com/locate/jtv)

## Clinical study

# Deep tissue injury rat model for pressure ulcer research on spinal cord injury

Fang Lin<sup>a,b,c</sup>, Atek Pandya<sup>a,b</sup>, Andrew Cichowski<sup>a,b</sup>, Mauli Modi<sup>b</sup>,  
 Briana Reprogle<sup>b</sup>, Dongkeun Lee<sup>b</sup>, Norio Kadono<sup>b</sup>,  
 Mohsen Makhsous<sup>a,b,c,d,\*</sup>

<sup>a</sup> Department of Sensory Motor Performance Program, Rehabilitation Institute of Chicago, 345 E. Superior Str. Suite 1406, Chicago, IL 60611, USA

<sup>b</sup> Department of Physical Therapy & Human Movement Sciences, Northwestern University, 645 N. Michigan Ave. Suite 1100, Chicago, IL 60611, USA

<sup>c</sup> Department of Physical Medicine & Rehabilitation, Northwestern University, 345 E. Superior Street, Chicago, IL 60611, USA

<sup>d</sup> Department of Orthopaedic Surgery, Northwestern University, 676 N. Saint Clair, Suite 1350, Chicago, IL 60611, USA

**KEYWORDS**

Spinal cord injury;  
 Deep tissue injury;  
 Animal model;  
 Implant;  
 Histology

**Abstract** Many rat/mouse pressure ulcer (PU) models have been developed to test different hypotheses to gain deeper understanding of various causative risk factors, the progress of PUs, and assessing effectiveness of potential treatment modalities. The recently emphasized deep tissue injury (DTI) mechanism for PU formation has received increased attention and several studies reported findings on newly developed DTI animal models. However, concerns exist for the clinical relevance and validity of these models, especially when the majority of the reported rat PU/DTI models were not built upon SCI animals and many of the DTI research did not simulate well the clinical observation. In this study, we propose a rat PU and DTI model which is more clinically relevant by including chronic SCI condition into the rat PU model and to simulate the role of bony prominence in DTI formation by using an implant on the bone–tissue interface. Histological data and imaging findings confirmed that the condition of chronic SCI had significant effect on pressure induced tissue injury in a rat PU model and the including a simulated bony prominence in rat DTI model resulted in significantly greater injury in deep muscle tissue. Further integration of the SCI condition and the

\* Corresponding author at: Department of Physical Therapy & Human Movement Sciences, Northwestern University, 645 N. Michigan Ave. Suite 1100, Chicago, IL 60611, USA. Tel.: +1 312 503 0073; fax: +1 312 908 0741.

E-mail address: [m-makhsous2@northwestern.edu](mailto:m-makhsous2@northwestern.edu) (M. Makhsous).

simulated bony prominence would result a rat PU/DTI model which can simulate even more accurately the clinical phenomenon and yield more clinically relevant findings.

© 2009 Tissue Viability Society. Published by Elsevier Ltd. All rights reserved.

## Introduction

Basic and preclinical research on pressure ulcers (PU) are usually carried out on animal models to gain deeper understanding of various causative risk factors, the progress of PUs, and assessing effectiveness of potential treatment modalities. Many animal PU models have been developed to test different hypotheses in this field [17,20] on several species, such as rat, dog, mouse, and pig. Although it is generally agreed that the pig is the ideal species for PU and wound healing research because of its fixed skin structure and cutaneous blood supply are similar to that in humans [26], the most commonly used animals in PU research are rats and mice possibly due to their easy handling and relatively low cost. A classic example of such model was the fuzzy rat model developed by Salcido et al. [19], on which a series of research has performed to elucidate the role of ischemia-reperfusion injury in PU formation. However, none of the reported rat PU models except one [15] was built upon SCI animals, while the majority of the studies claimed some relevance to PU formation in SCI population.

The development of PU animal models also reflects the specific understanding of the etiology of PU and the clinical observation of PU formation and healing. Deep tissue injury (DTI), as a recently emphasized mechanism for PU formation [3,5], has received increased attention lately and several studies reported findings on newly developed DTI animal models [7,22–24]. The clinical view of DTI emphasizes the severity of clinically identified DTI as that a true DTI progresses rapidly even with the most aggressive treatment [10] and its massive tissue necrosis is in a similar nature of a Stage-IV full-thickness wound [21]. However, current DTI animal researches have not reported findings resemble these descriptions. For example, none of DTI studies reported that the experimentally induced DTI eventually progressed to be an open wound which affected superficial skin, and the histological or imaging data of the induced DTI did not suggest massive tissue necrosis. Although it might be that most studies did not keep their DTI animals long enough to observe the formation of an open wound from the DTI, the results from our own observation and Kwan et al. [13], in which no skin lesion was formed after 7 days of DTI, do not support this

speculation. It may be that, in these DTI studies, the injured deep layer had healed, which suggested the DTI created in these models may not be as severe as the counterpart observed in clinic. Then the question raised is that how relevant these lab-created DTI to those observed in clinic, therefore, the clinical relevance of these DTI animal models has not yet been confirmed. By examination of the existing PU rat models, especially those for DTI research, we came to our assumption that the missing bony prominence may possibly be a drawback to prevent those models to yield more clinical relevant data. It has long been the understanding that PUs often occur at tissue pressure points around a bony prominence. We believe that, to more accurately simulate the clinical scenario of DTI formation, a bony prominence is necessary for a rat DTI model.

Therefore, we aimed in our study to establish a more clinically relevant rat PU model. The two objectives were to include SCI condition in a rat PU model and to simulate the role of bony prominence in DTI formation.

## Material and methods

Twenty-one female adult Sprague-Dawley rats, starting with 12–14 weeks old were used. Eight were used to establish the SCI/PU model (SCI), 8 were used as the PU model neurologically intact (Neuro-Intact) controls, and 5 were used for the implant-DTI model (Implant-DTI). Rats were housed under a normal light cycle and temperature of 23 °C. All procedures were approved by the ACUC of the institution.

### Surgical transection of the spinal cord for SCI model

After initial 2-week handling stage, rats in SCI group went through a complete transection of the spinal cord at T10 under general anesthesia of inhalation of 2–3.5% isoflurane mixed with oxygen. Through an incision along the spinal column, a laminectomy was performed for the T9 vertebra then the spinal cord was severed. To ensure a complete transection, 2~3 mm length of the cord tissue was cut and aspirated out of the spinal canal. Postoperatively, the rat was given analgesic

(Buprenex, 0.05 mg/kg, b.i.d) for 2 days and nonsteroidal anti-inflammatory Meloxicam (Metacam, 2 mg/kg, q.d) for 4–5 days and antibiotics (Baytril 5 mg/kg, b.i.d) for 7 days. Manual bladder expression was performed 3~4 times a day until automatic voidance of the bladder was established around 3–10 days post the surgery.

### Surgical placement of the simulated bony prominence for the DTI model

To simulate the role of a bony prominence in DTI formation, a hemispheric implant (diameter = 1.8 mm) with a short handle (Fig. 1 A) was placed for the Implant-DTI group of rats on the lateral surface of the right tibia bone and underneath the tibialis anterior (TA) muscle under general anesthesia. A 10 mm skin incision was made on the medial side of tibia to expose the anterior edge of the tibia. Through a small separation of the TA and the bone that extended across the width of the tibia, an implant was inserted underneath TA and tied tightly onto the tibia bone (Fig. 1B) before the incisions were closed using 4-0 suture. The right leg of the implant group of rats was surgically manipulated, while the left leg was left intact for a within-subject control. Postoperatively, the rat was given Buprenex (0.05 mg/kg, once) and Meloxicam (2 mg/kg, q.d for 2 days).

### Tissue compression for creating pressure injury

Tissue compression on TA muscle for inducing PU was performed at 6 weeks post SCI for SCI and Neuro-Intact groups, and 4 weeks post implant surgery for Implant-DTI group. Compression was delivered to the skin surface of the TA muscle at the location of the midpoint of the muscle belly. For Implant-DTI group, the applicator of the

compression was placed on the tissue on top of the implant. A custom apparatus for delivering the compression is shown in Fig. 2. The location of the compression can be precisely selected by adjusting the location and orientation of the applicator (indenter) longitudinally (proximal-distal) along the tibial shaft and rotationally around the tibia bone. The magnitude of the compression was controlled by adjusting the length of a compressed steel spring connected to the applicator. The spring was pre-calibrated using a load cell (ELFF-T4E-10L, Measurement Specialties, Inc, Fremont, CA, USA) and a caliper to obtain the force-length curve, and the compressive pressure applied to the tissue was obtained by converting the force to pressure over the area of the applicator (diameter = 3 mm).

For SCI/PU model, the compression was only applied to the left hindleg of both SCI and Neuro-Intact groups for 10 h of 400 mmHg, 2 h release followed by another 10 h of 400 mmHg. For DTI model, to test the effect of the simulated bony prominence, compression was applied to both hindlegs. As the DTI model was a prove-of-concept study and we attempted to find the most appropriate protocol, 3 different compression protocols were tested. For two animals, same protocol as in SCI/PU model was used but the pressure was reduced to 200 mmHg. For other two rats, 200 mmHg pressure was applied for 24 h, and for the rest one animal, 400 mmHg was applied for 24 h.

### MRI scan for soft tissue injury post compression

At day 7 after the compression, a T2 MRI scan was performed for rats in Implant-DTI group. The rats were anesthetized to provide a stable scan. T2 image sequences were obtained for bilateral shanks and the tissue injury was qualitatively examined.

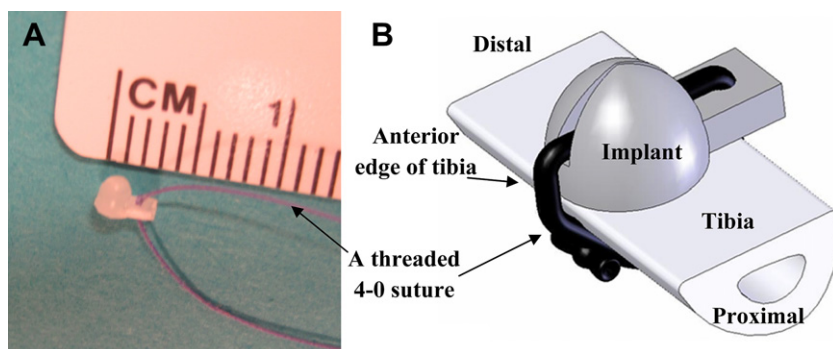
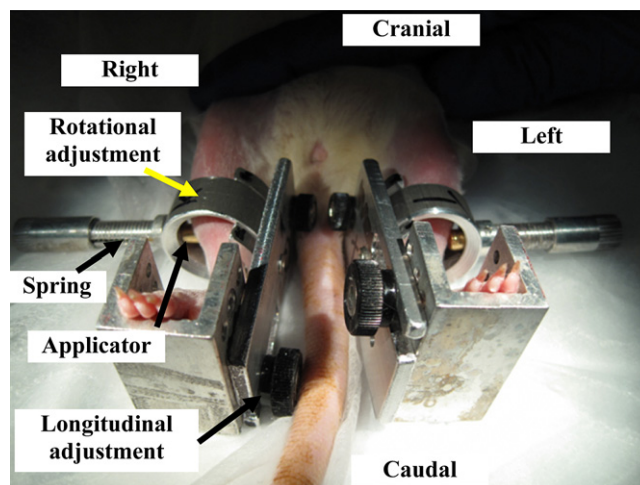


Figure 1 Implant (A) and its fixation method (B) used for the DTI model.



**Figure 2** Demonstration of the application of compression load to bilateral shanks of a rat.

### Tissue sample preparation and histological analysis

Seven days after the beginning of the compression, the animals were sacrificed using a transcardial perfusion with 4% paraformaldehyde following a rinse using neutral PBS solution with heparin. Both hindlegs were excised and stored in 4% paraformaldehyde solution for 2 weeks for postfixation. After the postfixation, the TA muscle was dissected from the legs and embedded in paraffin and then sliced at 5  $\mu\text{m}$  of thickness before stained using standard hematoxylin and eosin (H & E) protocol.

### Quantifying tissue involvement for pressure induced injury

Pressure induced muscle injury was quantified for its extent of tissue damage on cross sectional slides. Take the location of compression as the center the TA was harvested 6 mm maximal in distal and in proximal. The harvested muscle sample was bisected first along the longitudinal direction into a medial piece and a lateral piece. The medial piece was further bisected transversely at the center into a proximal portion and a distal portion. The total length of the proximal and distal portions was measured. Five cross sectional slides were then taken for both the proximal and distal portions at the distance of 0%, 25%, 50%, 75%, and 100% of its total length to the compression center. For the lateral portion of the TA muscle sample, 5 longitudinal slides were taken in the same manner relative to its thickness. Each slide was photographed through a microscope (AxioScope, Carl Zeiss MicroImaging, Inc., Thornwood, NY, USA). Due to limited view field under the microscope, multiple photos were taken for each slide to cover the entire

tissue sample. These photos were then assembled as a mosaic picture for each slide in Adobe Photoshop 7.0. The extent of tissue injury was quantified (Fig. 3) using a custom Matlab (Matlab R2009 a, The Mathworks, Inc., Natick, MA, USA) code. On each of the 10 cross sectional slides from a sample, the dimension of total area of the tissue and the area of the injured tissue were identified in  $\text{mm}^2$ , and the percentage of tissue injury was calculated as the percentage the injured tissue in the total area of the tissue. For each leg, the average total area of the tissue, the absolute area of injured tissue and the injury percentage on the 10 cross sectional slides were calculated as the measure of the extent of the muscle injury.

### Statistical analysis

Statistical analysis of the data was aimed at detecting the effect of SCI and the effect of bony prominence (Implant) on the extent of the pressure induced muscle injury. A two-sample *t*-test was performed on total area of tissue and the percentage of injury for SCI and Neuro-Intact groups to examine the effect of SCI. A one-sample *t*-test was performed on these measures on the Implant-DTI group of rats to examine any difference between the 2 legs, i.e. with and without implant. SPSS (SPSS 17.0, SPSS, Inc., Chicago, IL, USA) was used and a *P* value smaller than 0.05 was considered as significant.

### Results

All animals tolerated well the surgical procedure of SCI or implant placement. All rats in SCI group were in apparent paraplegia immediately post spinal cord

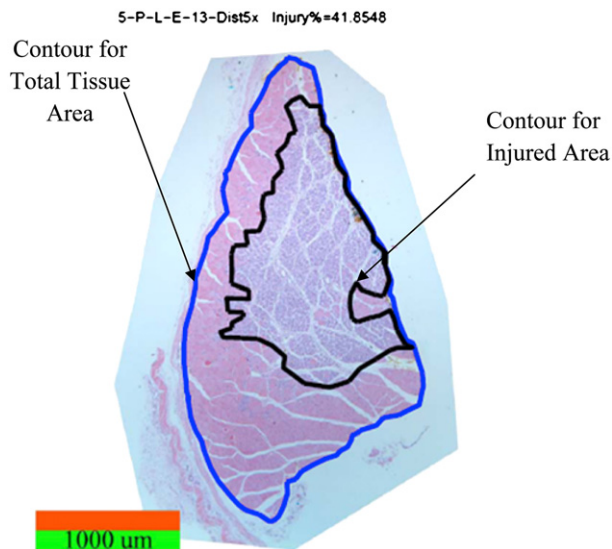


**Figure 3** A cross sectional slide (an assembled mosaic picture) is shown for the method of quantification of the extent of the pressure induced tissue injury. Stain: H & E. Image: 50× Magnification.

transection. Two to six weeks post SCI two rats showed symptoms of recovered voluntary motor function in hindlimbs, which were later confirmed by necropsy that there appeared a 40% and 60% connection at the transection site of their spinal cord. They were not excluded from the data analysis because incomplete SCI is commonly seen in clinic.

Postoperative ultrasound image (Fig. 4) taken 2 weeks after the implant surgery showed correct orientation of the implant on the bone. Photo taken at the time of tissue sample harvest (Fig. 5) confirmed the solid fixation of the implant onto the tibia bone and that the muscle wrapped neatly around the implant.

After the compression, a general injury progress pattern was observed. Immediately after the compression, there was an apparent shallow depression corresponding to the size and location of

the applicator. The shank of the compressed leg showed severe acute edema in a couple of hours after the compression. We observed the most severe edema in 24 h of the compression. After that, the tissue edema gradually resolved over the time and all edema was completely resolved in 48 h with a slight redness left at the site of compression. Three days post compression, tissue at the compressed location all showed normal appearance, except that one of the animals finally developed an open wound on one of its legs.

### Typical results for pressure induced injury shown on histological slides

A typical example of the pressure induced injury is shown in Fig. 6 for substantial differences between healthy and compression-injured tissue. On this slide, normal, healthy muscle fibers are stained as being more eosinophilic (Area I in Fig. 6). Interspersed amongst the healthy tissue are peripheral nuclei (Arrow 1 in Fig. 6), as in normal muscle anatomy, that stain darker [29]. Significant changes were seen at the injury site. Histological observation indicates that the effects of the compression are localized to the area of indentation (Area II). Darker stained areas show loss of fiber definition in comparison to healthy tissue, indicative of degeneration and skeletal muscle damage [4]. Damaged areas also show centralized nuclei (Arrow 2) and cellular phagocytotic infiltration (Arrow 3), both major indicators for post-damage regeneration [2,4,6,31]. In addition, the observed tissue necrosis shows damaged areas that are apparently displaced from the centralized injury area (Area III compared to area II). Furthermore, this displaced tissue necrosis does not simply appear in the distant area, as if another compression occurred, but moves along the fiber.

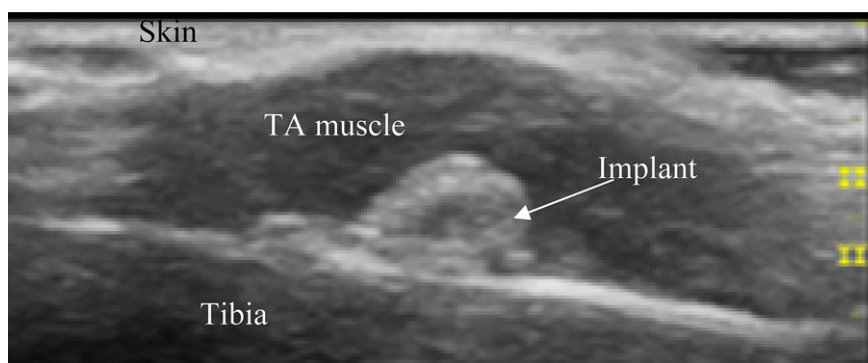


**Figure 4** B-mode ultrasound image showing the implant and the healed soft tissue 2 weeks post implant surgery.

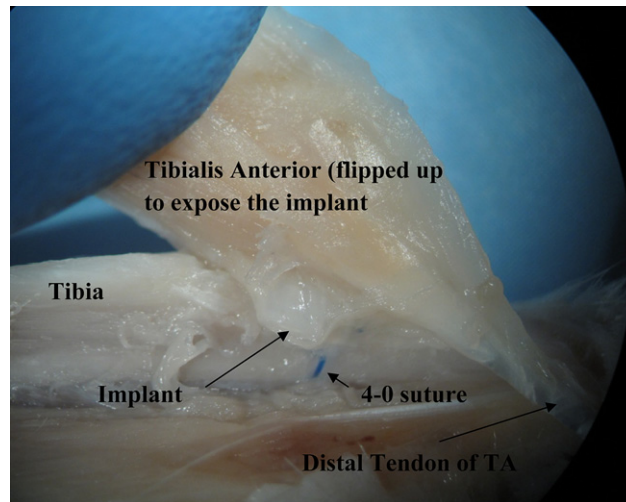


**Figure 5** A photo of dissection of the rat shank showing the implant fixation on the tibia bone and underneath the tibialis anterior muscle.

The most extreme tissue damage was seen from the right TA of an Implant-DTI rat, where an implant was inserted underneath the TA muscle and the shank was compressed with 400 mmHg for 24 h. Photo and histological image are shown for this case in Fig. 7. On this TA sample, a cavity (Marker I) is seen at approximately the center of the muscle and is enclosed entirely within the muscle. Therefore it is unlikely that this cavity was

caused by external laceration but through the applied compression and subsequent tissue necrosis. This lesion showed visible necrosis when dissected (Marker II) that was later confirmed by histological analysis (Fig. 7B). The large cavity was also surrounded by necrotic or heavily damaged tissue (Marker III), confirming that the cavity was most likely due to tissue breakdown versus an extraneous factor. Another finding of histological

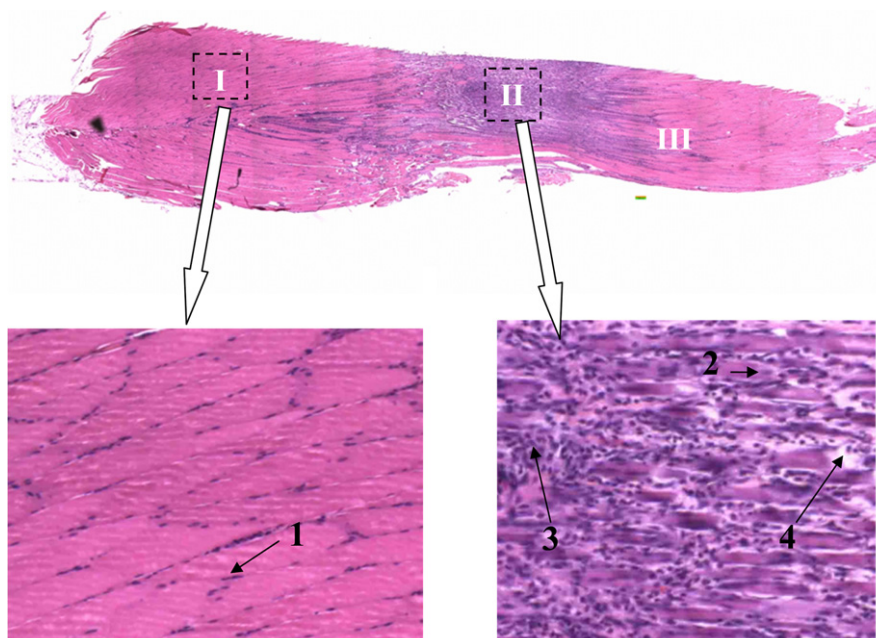


**Figure 6** A sample longitudinal section (an assembled mosaic picture) taken from a rat in Neuro-Intact group. Clear definitions between healthy tissue (I) and the injury area (II) can be seen. Normal fibers show peripheral nuclei (arrow 1). Darker areas show centralized nuclei (arrow 2), phagocytes infiltration (arrow 3) and degenerated fibers (arrow 4); all indicating tissue damage and repair. Further tissue damage is seen (III) away from the center of injury (II), indicating continuing tissue necrosis. Stain: H & E. Image: 50× Magnification.

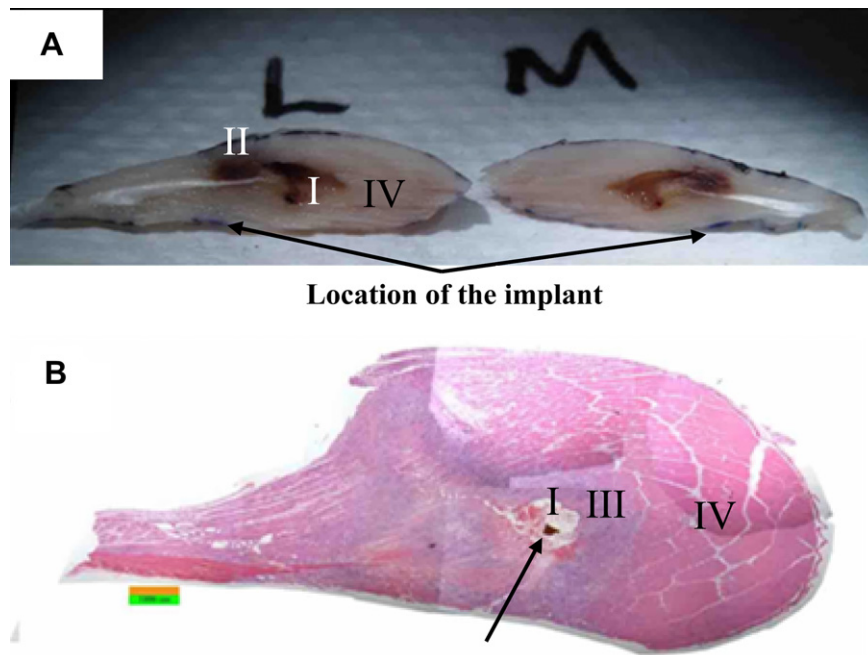


**Figure 7** An assembled mosaic picture for the most extreme tissue damage observed from the right TA of an Implant-DTI rat with compression of 400 mmHg of 24 h. Figure A shows a photograph of the dissected TA. The muscle was bisected longitudinally to reveal the formed deep pressure ulcer. The lateral side (L) and the medial side (M) of the TA both show an evenly distributed cavity that clearly shows necrotic tissue at and distal to the lesion (I and II) and healthy tissue (IV) proximal to the cavity. Figure B is a longitudinal section from the same TA that also shows the formation of the deep ulcer (I) as well as heavily damaged (III) and healthy tissues (IV). Histology observation also shows a calcification possibly due to extreme damage to the muscle tissue (arrow). Stain: H & E. Image: 50× Magnification.

analysis for this case was a small calcification (arrow) very near the cavity, which has been previously shown to be a resultant of traumatic soft tissue injury [28]. Like many other compressed tissues, this case also showed healthy peripheral tissue (Marker IV) mainly proximal to the lesion, but nevertheless had a significant void which is decidedly a deep pressure ulcer formation.

#### Typical results for pressure induced injury shown on MRI images

A typical example of the pressure induced injury observed in MRI imaging is shown in Fig. 8 for difference of the tissue damage on the shanks of the same rat. The TA on the right side, where the implant was placed, had a substantial amount of tissue damage at 7 days post compression. The tissue damage seen on MRI was mostly in the muscle and some was in subcutaneous tissue while the skin remained intact. The visual observation for this rat did not find any skin lesion at this time. On MRI scan, there was no tissue injury in left (no-implant) TA which was later confirmed on the histological slides from the same sample.

#### Average results for the SCI effect

Body weight of the SCI and Neuro-Intact groups of rats were  $260.6 \pm 28.5$  g and  $257.2 \pm 15.7$  g ( $P > 0.05$ ), respectively at the start of the study and were  $269.2 \pm 31.7$  g and  $299.4 \pm 27.6$  g ( $P = 0.031$ ),

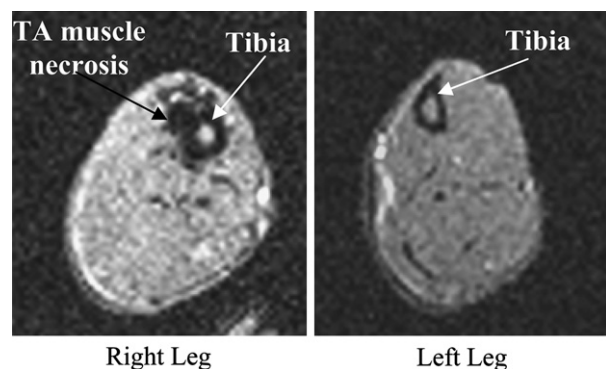


**Figure 8** Axial MRI images for the same rat 7 days post compression. Left: Leg with implant, massive tissue damage remained and superficial tissue started to be involved; Right: without implant. Tissue damage did not present possibly due to effective healing.

respectively at the end of the study. Over the 8 weeks of the study, body weight increase was significantly lower in the SCI animals ( $P = 0.008$ ). The average total tissue area, tissue injury area and the injury percentage are given in Table 1 for SCI and Neuro-Intact groups. The Neuro-Intact rats had significantly larger total area of tissue ( $P = 0.004$ ) which corresponds to a significantly greater body weight. While the percentage of tissue injury was significantly greater in SCI rats ( $P = 0.001$ ), the absolute injury area, although substantially greater in SCI group, did not show statistical significance between the groups.

### Average results for the simulated bony prominence effect

The average total tissue area, tissue injury area and the injury percentage are given in Table 1 for the Implant-DTI group in comparison between the right (Implant side) and left (No-Implant side) hindlegs. There was no significant difference between the two sides of the hindlegs in total area of tissue ( $P > 0.05$ ), while both the absolute injury area and the percentage of tissue injury were significantly greater on implant side, with  $P$ -values of 0.041 and 0.031, respectively.

## Discussion

This study reports a rat model for pressure ulcers in SCI condition and a version of such model aiming at generating clinically relevant pressure induced deep tissue injury. Results from the experiment and subsequent histological analysis and MRI imaging observation confirmed that these models are successful in simulating the said clinical conditions.

Numerous animal models have been established in this research field [17,20] for investigating various theories on etiological factors of PU

formation, observing wound formation and healing, and assessing treatment modalities. Great progress has been achieved on PU animal research during the last 2 decades and precious knowledge has been acquired from these animal models, which has fostered the advances in recent PU basic research and clinical practice. However, several weaknesses may prevent these animal models to be the best for researches on PUs specifically for SCI condition or for research focusing on the DTI. Since the philosophy of carrying out research on animal models is to obtain knowledge under well controlled experimental condition which simulates the clinical scenario the problem occurs, the ability of generating such knowledge depends on how well the animal models mimic the relevant clinical conditions that generate the PUs [20]. From this point of view, a quick concern is that the majority of the reported animals PU models lack one critical factor, spinal cord injury. Although PUs do occur in individuals without SCI, the major research and practice effort are directed towards the care of SCI population for PU management because the 33% [1] prevalence of PU in this population. Therefore, an animal model for PU research for SCI condition should be designed with the factor of SCI in consideration. But the current situation is that PU animal models involving SCI or denervation of part of the body are rare and have been almost exclusively established on large animals, such as pigs. In his classic work, Dinsdale presented a swine PU model using paraplegic pigs [9]. Daniel et al. also created PU by compressing tissue at greater trochanter of paralyzed pigs [8]. Hyodo A et al reported a monoplegic PU model on minipigs [12].

Before the current study, one of the very few, if not the only one, rat models for PU research which had been established on SCI animals was from Li et al [15]. In their study, Li et al evaluated the response of skin blood flow to prolonged pressure loading of 100 mmHg for 6 h in SCI and non-SCI rats.

**Table 1** The total area of tissue ( $\text{mm}^2$ ), total area of injury ( $\text{mm}^2$ ), and injury percentage (%) in SCI/PU and Implant-DTI models for SCI, Neuro-Intact, Implant groups (Mean  $\pm$  SE). The  $P$ -values are given for comparison between the SCI and Neuro-Intact groups (P1) and between the No-implant and Implant legs (P2) with a significant level of 0.05.

| Model           | Total area of tissue ( $\text{mm}^2$ ) | Total area of injury ( $\text{mm}^2$ ) | Injury percentage (%) |
|-----------------|--|--|-----------------------|
| SCI/PU:         |  |  |                       |
| Neuro-Intact    | 88.7 $\pm$ 14.8                        | 9.9 $\pm$ 1.7                          | 17.2 $\pm$ 10.0       |
| SCI             | 44.0 $\pm$ 9.7                         | 20.6 $\pm$ 6.2                         | 54.0 $\pm$ 10.8       |
| P1              | <b>0.004</b>                           | >0.05                                  | <b>0.001</b>          |
| Implant-DTI:    |  |  |                       |
| No-implant side | 66.0 $\pm$ 6.2                         | 8.5 $\pm$ 7.1                          | 10.6 $\pm$ 8.7        |
| Implant side    | 72.1 $\pm$ 4.2                         | 26.4 $\pm$ 2.5                         | 42.6 $\pm$ 6.2        |
| P2              | >0.05                                  | <b>0.041</b>                           | <b>0.031</b>          |

They reported significantly compromised hyperemic response of the skin blood flow in the neurogenic region of Laser Doppler Flowmetry in SCI rats, in comparison to normal controls. Li's report further confirmed our concern that animals in SCI condition respond to pressure injury in a different pattern than that of the neurologically intact animals, therefore, emphasized the needs to conduct PU related animal research on an animal model which possesses the concerned pathophysiological condition, which in this case, spinal cord injury. However, it should be pointed out that this single SCI rat PU model may have some controversy in that their creation of SCI was a unilateral hemisection of spinal cord at C7 [30] while their observation of tissue injury and blood flow was performed bilaterally at trochanter [14]. Another concern for this SCI rat model is that there was no clear description whether the SCI condition was acute or chronic.

The second objective for the current study was to create deep tissue injury using a simulated bony prominence. It has long been the understanding that pressure ulcers often occur at tissue pressure points around a bony prominence. Latest simulation approaches have revealed substantially concentrated stress and deformation around internal bony prominences [16], which were thought to contribute to tissue damage in the deep layers such as muscle. However, current DTI related animal research has not addressed this issue effectively. While some animal models used the locations of natural bony prominences such as scapula [11] and femoral trochanter [13], many other studies simply applied load to tissues with no bony prominence presented, such as tibialis anterior. Tissue over scapula and trochanter is generally thin and contains very little muscle tissue while deep muscle injury is the focus for deep tissue injury research.

The only animal model aiming at creating stage-IV PU was from Wassermann et al [27]. Wassermann et al used an implanted metal plate underneath the great gluteus muscle while the compression between an external plate and this internal plate successfully created full-thickness lesions involving muscle tissues. However, while the deep tissue injury created by this method seemed clinical relevant, there exist some concerns. While the two plates compress the full-thickness of the soft tissue in between them, the pulling force on the internal plate will inevitably pull the deep tissue in the direction away from deeper tissue or the bone, adding additional tissue damaging factors. Therefore, the damage of the deep tissue in this model involves additional mechanism which is not usually seen in clinical

scenario such as tissue compression due to unrelied compressive pressure. Our current model solves this problem by placing an implant onto the tibia bone to simulate the exact situation of a natural bony prominence. Not only the shape of the implant resembles that of the ischial tuberosity, but the subsequent compression on top of the implant simulates the natural loading scenario of sitting. Another study by Sari et al. [22] was successful in creating an full-thickness open wound. However, the compression load applied to the tissue in this study was over 2000 mmHg, which is highly irrelevant to practical situation.

Quite several PU animal models have been developed using techniques that compressed skin without involving deep muscles [18,25]. While it may be an excellent way to study details for skin lesion formation and healing, it hardly can be claimed as "clinically relevant" while in clinical reality, it is rare to see a load applies to skin only without getting the subcutaneous and even deeper layers involved.

The limitation of the current study is that the Implant-DTI group contains very limited number of animals at the current stage. Since this is a prove-of-concept study for this specific objective, we believe the obtained data clearly support the model design of using an implant to simulate a bony prominence. However, more animals need to be tested for a final prove that this model is successful.

## Conclusions

In comparison to existing animal models, the reported rat models in the current study have the advantages in simulating PU formation in SCI condition and the DTI formation around bony prominence. Histological data and imaging evidence support the claims. Our further work will be to implement the Implant-DTI model in SCI animals and carry out researches on these models.

## Conflict of interest

The authors have no conflict of interest that could inappropriately influence the study.

## Acknowledgements

The project was supported in part by NIH Award K25 #HD051983-01A (Makhsous). The authors are

grateful for Dr. Todd Parrish for generous help in MRI scanning; Dr. Lin Li and Donna J. Emge, ASCP-HT for their help in histological evaluation and data processing; and Mr. Di Zhang and Mr. Mike Bajema for their help in fabrication of the compression apparatus.

## References

- [1] National Spinal Cord Injury Statistical Center. 2006 Annual report for model spinal cord injury care systems. Edited. Birmingham, AL: University of Alabama; 2006.
- [2] Abraham ST, Shaw C. Increased expression of deltaCaMKII isoforms in skeletal muscle regeneration: implications in dystrophic muscle disease. *J Cell Biochem* 2006;97(3): 621–32.
- [3] Ankrom MA, Bennett RG, Sprigle S, Langemo D, Black JM, Berlowitz DR, et al. Pressure-related deep tissue injury under intact skin and the current pressure ulcer staging systems. *Adv Skin Wound Care* 2005;18(1):35–42.
- [4] Armstrong RB, Ogilvie RW, Schwane JA. Eccentric exercise-induced injury to rat skeletal muscle. *J Appl Physiol* 1983; 54(1):80–93.
- [5] Black J, Baharestani MM, Cuddigan J, Dorner B, Edsberg L, Langemo D, et al. National Pressure Ulcer Advisory Panel's updated pressure ulcer staging system. *Adv Skin Wound Care* 2007;20(5):269–74.
- [6] Bronneberg D, Spiekstra SW, Cornelissen LH, Oomens CWJ, Gibbs S, Baaijens FPT, et al. Cytokine and chemokine release upon prolonged mechanical loading of the epidermis. *Exp Dermatol* 2007;16(7):567–73.
- [7] Ceelen KK, Stekelenburg A, Loerakker S, Strijkers GJ, Bader DL, Nicolay K, et al. Compression-induced damage and internal tissue strains are related. *J Biomech* 2008; 41(16):3399–404.
- [8] Daniel RK, Priest DL, Wheatley DC. Etiologic factors in pressure sores: an experimental model. *Arch Phys Med Rehabil* 1981;62(10):492–8.
- [9] Dinsdale SM. Decubitus ulcers in swine: light and electron microscopy study of pathogenesis. *Arch Phys Med Rehabil* 1973;54(2):51–6.
- [10] Farid KJ. Applying observations from forensic science to understanding the development of pressure ulcers. *Ostomy Wound Manage* 2007;53(4).
- [11] Hagiwara S, Ferguson-Pell MW, Palmieri VR, Cochran GV. Pressure sores: a biochemical test for early detection of tissue damage. *Arch Phys Med Rehabil* 1988;69(9):668–71.
- [12] Hyodo A, Reger SI, Negami S, Kambic H, Reyes E, Browne EZ. Evaluation of a pressure sore model using monoplegic pigs. *Plast Reconstr Surg* 1995;96(2):421–8.
- [13] Kwan MPC, Tam EWC, Lo SCL, Leung MCP, Lau RYC. The time effect of pressure on tissue viability: investigation using an experimental rat model. *Exp Biol Med* 2007; 232(4):481–7.
- [14] Li Z, Tam EWC, Kwan MPC, Mak AFT, Lo SCL, Leung MCP. Effects of prolonged surface pressure on the skin blood flowmotions in anaesthetized rats—an assessment by spectral analysis of laser Doppler flowmetry signals. *Phys Med Biol* 2006;51(10):2681–94.
- [15] Li Z, Tam EWC, Lau RYC, So K-F, Wu W, Mak AFT. Post pressure response of skin blood flowmotions in anesthetized rats with spinal cord injury. *Microvasc Res* 2009; 78(1):20–4.
- [16] Makhosous M, Lim D, Hendrix RW, Bankard J, Rymer WZ, Lin F. Finite element analysis for evaluation of pressure ulcer on the buttock: development and validation. *IEEE Trans Neural Syst Rehabil Eng* 2007;15(4):517–25.
- [17] Nguyen PK, Smith AL, Reynolds KJ. A literature review of different pressure ulcer models from 1942–2005 and the development of an ideal animal model. *Australas Phys Eng Sci Med* 2008;31(3):223–5.
- [18] Peirce SM, Skalak TC, Rodeheaver GT. Ischemia-reperfusion injury in chronic pressure ulcer formation: a skin model in the rat. *Wound Repair Regen* 2000; 8(1):68–76.
- [19] Salcido R, Donofrio JC, Fisher SB, LeGrand EK, Dickey K, Carney JM, et al. Histopathology of pressure ulcers as a result of sequential computer-controlled pressure sessions in a fuzzy rat model. *Adv Wound Care* 1994;7(5): 23–4. 26, 28 passim.
- [20] Salcido R, Popescu A, Ahn C. Animal models in pressure ulcer research. *J Spinal Cord Med* 2007;30(2):107–16.
- [21] Salcido RS. Myosubcutaneous infarct: deep tissue injury. *Adv Skin Wound Care* 2007;20(5):248–50.
- [22] Sari Y, Nakagami G, Kinoshita A, Huang L, Ueda K, Iizaka S, et al. Changes in serum and exudate creatine phosphokinase concentrations as an indicator of deep tissue injury: a pilot study. *Int Wound J* 2008;5(5):674–80.
- [23] Siu PM, Tam EW, Teng BT, Pei XM, Ng JW, Benzie IF, et al. Muscle apoptosis is induced in pressure-induced deep tissue injury. *J Appl Physiol* 2009. 90897.2008.
- [24] Solis LR, Hallihan DP, Uwiera RRE, Thompson RB, Pehowich ED, Mushahwar VK. Prevention of pressure-induced deep tissue injury using intermittent electrical stimulation. *J Appl Physiol* 2007;102(5):1992–2001.
- [25] Stadler I, Zhang RY, Oskoui P, Whittaker MS, Lanzafame RJ. Development of a simple, noninvasive, clinically relevant model of pressure ulcers in the mouse. *J Invest Surg* 2004; 17(4):221–7.
- [26] Swindle MM. Swine in the laboratory: surgery, anesthesia, imaging, and experimental techniques. Edited. Boca Raton: CRC Press, Taylor & Francis Group; 2007.
- [27] Wassermann E, Mv Griensven, Gestaltner K, Oehlinger W, Schrei K, Redl H. A chronic pressure ulcer model in the nude mouse. *Wound Repair Regen* 2009;17(4):480–4.
- [28] William HM, Glen KA, William ES, Henry HB. The acute calcification of traumatized muscle, with particular reference to acute post-traumatic renal insufficiency. *J Clin Invest* 1957;36(6 Part 1):825–32.
- [29] Wolfgang K. Color atlas of cytology, histology, and microscopic anatomy. Edited. Stuttgart: Georg Thieme Verlag; 2003.
- [30] Yick L-W, So K-F, Cheung P-T, Wu W-T. Lithium chloride reinforces the regeneration-promoting effect of chondroitinase ABC on rubrospinal neurons after spinal cord injury. *J Neurotrauma* 2004;21(7):932–43.
- [31] Zulloff-Shani A, Kachel E, Frenkel O, Orenstein A, Shinar E, Danon D. Macrophage suspensions prepared from a blood unit for treatment of refractory human ulcers. *Transfus Apher Sci* 2004;30(2):163–7.